Superexchange Metal–Metal Coupling in Dinuclear Pentaammineruthenium Complexes Incorporating a 1,4-Dicyanamidobenzene Dianion Bridging Ligand

M. A. S. Aquino,[†] F. L. Lee,[‡] E. J. Gabe,[‡] C. Bensimon,[‡] J. E. Greedan,[§] and R. J. Crutchley*,[†]

Contribution from the Ottawa-Carleton Chemistry Institute, Carleton University, Ottawa, Canada K1S 5B6, the National Research Council of Canada, Chemistry Division, Ottawa, Canada K1A 0R6, and McMaster University, Institute for Materials Research, Hamilton, Ontario, Canada L8S 4M1. Received September 25, 1991

Abstract: Four dinuclear complexes, {μ-Dicyd-[(NH$_3$)$_5$Ru]$_2$}[ClO$_4$]$_4$ (1), {μ-Me$_2$Dicyd-[(NH$_3$)$_5$Ru]$_2$}[ClO$_4$]$_4$ (2), {μ-Cl$_2$Dicyd-[(NH$_3$)$_5$Ru]$_2$}[Cl]$_4$ (3), and {μ-Cl$_4$Dicyd-[(NH$_3$)$_5$Ru]$_2$}[Cl]$_4$ (4) where Dicyd^{2-} = 1,4-dicyanamidobenzene dianion, Me$_2$Dicyd^{2-} = 1,4-dicyanamido-2,5-dimethylbenzene dianion, Cl$_2$Dicyd^{2-} = 1,4-dicyanamido-2,5-dichlorobenzene dianion, and Cl$_4$Dicyd^{2-} = 1,4-dicyanamido-2,3,5,6-tetrachlorobenzene dianion, have been synthesized. A crystal structure of the tosylate salt of 1 was determined. Two conformations of the dinuclear complex were revealed in the unit cell. For conformer **A**, both Ru(III)–cyanamide bonds are essentially linear, having a Ru(1)–N(6)–C(1) bond angle of 175°. For conformer **B**, both Ru(III)–cyanamide bonds are bent, having a corresponding bond angle of 150°. In both conformers, the Dicyd^{2-} bridging ligand is planar with the cyanamide groups in an anti configuration. Crystal structure data for the complex are space group $P2_1/a$, with a, b, and c = 7.5861 (6), 23.0450 (19), and 32.078 (3) Å, respectively, $β$ = 95.771 (7)°, V = 5579.5 Å^3, and Z = 4. The structure was refined using 3947 significant Cu (1.54056 Å) reflections to an R factor of 0.063. The dinuclear complexes were characterized by cyclic voltammetry, UV–vis NIR spectroscopy, and magnetic susceptibility. The mixed-valence complexes [Ru(III), Ru(II)] of 1–4 were shown to be weak coupling cases with the order of coupling inferred from comproportionation constants at **1 < 4 < 3 < 2**. Temperature dependent magnetic susceptibility measurements of the oxidized complexes [Ru(III), Ru(III)] of 1–4 showed antiferromagnetic behavior. Isotropic spin only models of the data for **3** and **4** and the tosylate salt of **1** derived magnetic exchange coupling constants of J = −95.9, −61.9, and −100 cm^{-1}, respectively (where $\mathcal{H}$ = −2J$\vec{S}_a$·$\vec{S}_b$). For the perchlorate salt of **1**, a slight rise in magnetic susceptibility as temperature approached 300 K allowed an estimate of J ≥ −400 cm^{-1}. For **2**, antiferromagnetic coupling was of sufficient magnitude to render the complex diamagnetic at room temperature. Antiferromagnetic coupling of this magnitude at an estimated through space separation of 13.2 Å is unprecedented. Coupling in both mixed-valence and oxidized complexes is suggested to be dominated by a superexchange mechanism involving the Ru(III) dπ-orbitals and the π HOMO of the Dicyd^{2-} bridging ligand. Extended Huckel calculations have been performed using the crystal structure data of the free Dicyd^{2-} ligands to illustrate that a continuous π interaction between metal ions is possible.

Introduction

The purposeful synthesis of novel magnetic or electronic solid state materials requires a fundamental grasp of the underlying *molecular* properties of the unit building blocks that make up the crystal lattice. The goal is to be able to design the properties of a molecular unit and to assemble these units in a manner which expresses the desired *macroscopic* property. This idea is not new, but the design of molecular units that express potentially useful molecular properties is a field with considerable potential for development requiring contributions from all fields of chemistry and has additional application to the construction of molecular electronic devices.[1]

One strategy for the construction of a magnetic material has been to assemble molecular units composed of heterodinuclear complexes with total spin $S > 0$ in which the metal ions are antiferromagnetically coupled.[2] Room temperature magnetism requires that coupling between metal ions within molecular units and between molecular units be of sufficient magnitude to prevent randomization of spin. It is therefore essential that the means

by which metal–metal coupling can be propagated be fully explored to provide the optimum parameters for molecular unit design and synthesis.

The weak coupling of two metal ions bridged by a ligand has been long ascribed to a superexchange mechanism[3,4] in which metal ion states are mixed by virtual electronic states of the bridging ligand. These virtual states can be conceptualized as ones in which the bridging ligand can be either reduced (electron-type) or oxidized (hole-type). Consistent with the weak coupling of metal ions and the treatment of these systems by perturbation theory,[4,5] neither electron nor hole should be thought of as vibronically localized on the bridge. The bridge molecular

---

(1) (a) *Molecular Electronic Devices II*; Carter, F. L., Ed.; Marcel Dekker: New York, 1987. (b) *Molecular Electronics: Science and Technology*; Aviram, A., Ed.; Engineering Foundation: New York, 1989. (c) Beratan, D. N. *Mol. Cryst. Liq. Cryst.* **1989**, *190*, 85.

(2) For example, see: Kahn, O.; Pei, Y.; Verdaguer, M.; Renard, J. P.; Sletten, J. *J. Am. Chem. Soc.* **1988**, *110*, 782. Pei, Y.; Kahn, O.; Nakatani, K.; Codjovi, E.; Mathoniere, C.; Sletten, J. *J. Am. Chem. Soc.* **1991**, *113*, 6558 and references therein.

(3) Kramers, H. A. *Physica* **1934**, *1*, 182.

(4) McConnell, H. M. *J. Chem. Phys.* **1961**, *35*, 508.

(5) Kosloff, R.; Ratner, M. A. *Isr. J. Chem.* **1990**, *30*, 45.

orbital pathway should be continuous and shared by both metal ions with electron-type superexchange utilizing unoccupied molecular orbitals while that for hole-type superexchange utilizing occupied molecular orbitals. The magnitude of metal–metal coupling depends to a large extent on the magnitude of a given metal ion's interaction with the molecular orbitals involved in superexchange. A strong interaction between metal and ligand should give rise to electronic transitions. In particular, we have shown in previous studies[6,7] that it is possible to relate the oscillator strength of a ligand to metal charge transfer band to variations in the overlap integral between metal and ligand orbitals.

In this study, we examine the metal–metal superexchange coupling of ruthenium ions in dinuclear pentaammineruthenium complexes that incorporate the bridging ligand, 1,4-dicyanamidobenzene dianion (Dicyd^{2-}) and its derivatives. These bridging ligands are easily oxidized π-donor aromatic systems and when used respectively to bridged two Ru(III) π-acceptor ions in an oxidized [Ru(III),Ru(III)] dinuclear complex, significant superexchange coupling of the Ru(III) πd-orbitals is expected via the continuous π HOMO of the Dicyd^{2-} derivative. A similar pathway ought to be in effect for metal–metal coupling in the corresponding mixed-valence [Ru(III),Ru(II)] complexes. This represents a novel opportunity to experimentally investigate metal–metal coupling using both magnetic and electronic methods. Before we can present the synthesis, characterization, and physical properties of these molecular systems, we must first compare the treatments of metal–metal coupling derived from magnetic data and metal–metal charge transfer (MMCT) band properties.

The magnetic interaction between spins $\vec{S}_a$ and $\vec{S}_b$ for atoms **A** and **B** is usually written[8]

$$\mathcal{H} = -2J\vec{S}_a \cdot \vec{S}_b \qquad (1)$$

where the exchange coupling constant J is positive if the spins are parallel and negative if they are paired. In this study, two low spin Ru(III) ions with $S = 1/2$,[9] are coupled resulting in singlet and triplet states separated in energy by $-2J$. Magnetic exchange interactions between metal ions have been interpreted by using parameters which reflect the extent of electron exchange stabilization[10,11] and/or the extent of overlap[12] between coupled metal ion orbitals. Here we shall use the simple perturbation theory approach.

For the weak magnetic interaction of two 1/2 spins in orthogonal orbitals ϕ_a and ϕ_b, perturbation theory yields[10]

$$2J = K_{ab} - (2H_{ab}^2)/J_{aa} - J_{ab} \qquad \text{in cm}^{-1} \qquad (2)$$

The ferromagnetic term K_{ab} is the potential exchange integral and represents the overall spin pairing energy. The antiferromagnetic term is made up of the electron exchange integral H_{ab}, and the difference between coulomb repulsion integrals J_{aa} and J_{ab} which represents the energy required to place both spins on the same atom. This expression is similar to Anderson's treatment of superexchange in insulators which was based on an unrestricted Hartree–Fock formalism.[11]

For weakly coupled mixed-valence metal ions, the perturbation theory approach of the Hush model[13,14] accounts for the degree of electronic coupling between donor and acceptor wave functions by using information derived from the MMCT oscillator strength

$$H_{ad} = \frac{2.05 \times 10^{-2}}{R}(\epsilon_{max} \cdot \bar{\nu}_{1/2} \cdot \bar{\nu})^{1/2} \qquad (3)$$

where H_{ad} is the electron exchange integral in cm^{-1}, R is the separation between donor and acceptor wave functions in Å, ϵ_{max} is the maximum extinction coefficient of the MMCT band in M^{-1} cm^{-1}, $\bar{\nu}_{1/2}$ is the band width in cm^{-1} at one-half ϵ_{max}, and $\bar{\nu}$ is the energy of the MMCT transition at ϵ_{max} in cm^{-1}.

In special circumstances in which both donor and acceptor are paramagnetic, the values of H_{ab} and H_{ad} will be equivalent.[15] Indeed for a symmetric species (free energy for electron transfer = 0), the energy of the MMCT band will equal the value of $J_{aa} - J_{ab}$.[15,16] As will be shown, this is clearly not applicable to the mixed-valence [Ru(III), Ru(II)] and oxidized [Ru(III), Ru(III)] complexes of this study. However, the trends in H_{ab} and H_{ad} determined for the dinuclear complexes should be comparable provided the superexchange pathways are basically the same.

Experimental Section

Physical Measurements. UV–vis spectra were taken on a Perkin-Elmer Lambda 4b spectrophotometer. The NIR region was monitored using Cary 14 and Cary 5 spectrophotometers. Equipment used to perform cyclic voltammetry has been previously described.[17] Nonaqueous cyclic voltammetry was performed in dry acetonitrile[18] (0.1 M tetrabutylammonium hexafluorophosphate, TBAH), at 25 °C, with a three-electrode system consisting of platinum-disk working (BAS 1.6 mm diameter), and wire counter electrodes, and a silver wire quasi-reference electrode. Ferrocene ($E° = 400$ mV vs NHE)[19] was used as an internal reference. Aqueous cyclic voltammetry was performed in distilled water (0.1 M NaCl), at 25 °C, with a three-electrode system consisting of glassy carbon working (BAS 5-mm diameter), a platinum wire counter, and saturated calomel reference electrodes. Elemental analysis was performed by Canadian Microanalytical Services Ltd. Temperature dependent magnetic susceptibility measurements were performed on a Quantum Design S.Q.U.I.D. magnetometer from 5 to 300 K in a 1.0 T field.

Materials. All chemicals and solvents were reagent grade or better. Tetraphenylarsonium chloride monohydrate (Strem) was used as received. TBAH (Aldrich) was recrystallized twice from ethanol/water and vacuum dried at 118 °C. [(NH$_3$)$_5$RuCl][Cl]$_2$[20] and [(NH$_3$)$_5$Ru(OH$_2$)][PF$_6$]$_2$[21] were prepared by literature methods. The preparation of the tetraphenylarsonium salt of 1,4-dicyanamide-2,3,5,6-tetrachlorobenzene dianion (Cl$_4$Dicyd^{2-}) and complex **4** has been described in a preliminary paper.[22] 2,5-Dimethylphenylenediamine, 2,5-dichlorophenylenediamine and phenylenediamine (Aldrich) were used without further purification.

Preparation of 1,4-Dicyanamidobenzene Derivatives. The syntheses of the tetraphenylarsonium salts of 1,4-dicyanamidobenzene dianion (Dicyd^{2-}), 1,4-dicyanamido-2,5-dimethylbenzene dianion (Me$_2$Dicyd^{2-}), and 1,4-dicyanamido-2,5-dichlorobenzene dianion (Cl$_2$Dicyd^{2-}) follow essentially identical procedures. Unlike the tetrachloro derivatives, these ligands can be isolated analytically pure in their neutral protonated form. However, care should be taken during synthesis not to overheat the dianion form of the ligand in solution and to neutralize the aqueous solution rapidly. This is done to limit the tendency of phenylcyanamides to undergo autopolymerization.[23]

(6) Crutchley, R. J.; McCaw, K.; Lee, F. L.; Gabe, E. J. *Inorg. Chem.* **1990**, *29*, 2576.

(7) (a) Saleh, A. A.; Crutchley, R. J. *Inorg. Chem.* **1990**, *29*, 2132. (b) Crutchley, R. J.; Saleh, A. A.; McCaw, K.; Aquino, M. A. S. *Mol. Cryst. Liq. Cryst.* **1991**, *194*, 93.

(8) (a) Dirac, P. A. *Proc. R. Soc. London, Ser. A* **1929**, *123*, 714. (b) Heisenberg, W. *Z. Phys.* **1926**, *38*, 411; **1928**, *49*, 619. (c) van Vleck, J. H. *Theory of Electric and Magnetic Susceptibilities*; Oxford University Press: London, 1932.

(9) Experimental magnetic moments for low spin Ru(III) complexes range from 1.9 to 2.07 μ_B, suggesting that a close to spin only treatment is sufficient with only a small contribution from angular momentum. See: Figgis, B. N.; Lewis, J. *Prog. Inorg. Chem.* **1964**, *6*, 173.

(10) Hay, J. P.; Thibeault, J. C.; Hoffmann, R. *J. Am. Chem. Soc.* **1975**, *97*, 4884.

(11) Anderson, P. W. *Phys. Rev.* **1959**, *115*, 2.

(12) (a) Kahn, O.; Briat, B. *J. Chem. Soc., Faraday II* **1976**, *72*, 268 and 1441. (b) Kahn, O. In *Magneto-Structural Correlations in Exchange Coupled Systems*; Willet, R. D., Gatteschi, D., Kahn, O., Eds.; Reidel: Dordrecht, Holland, 1985; p 37.

(13) Hush, N. S. *Prog. Inorg. Chem.* **1967**, *8*, 391.

(14) Creutz, C. *Prog. Inorg. Chem.* **1983**, *30*, 1.

(15) (a) Okamura, M. Y.; Fredkin, D. R.; Isaacson, R. A.; Feher, G. In *Tunneling in Biological Systems*; Chance, B., De Vault, D. C., Frauenfelder, H., Marcus, R. A., Schrieffer, J. R., Sutin, N., Eds.; Academic Press: New York, 1974; p 729. (b) Bertrand, P. *Chem. Phys. Lett.* **1985**, *113*, 104.

(16) Hale, P. D.; Ratner, M. A.; Hofacker, G. L. *Chem. Phys. Lett.* **1985**, *119*, 264.

(17) Crutchley, R. J.; Naklicki, M. L. *Inorg. Chem.* **1989**, *28*, 1955.

(18) Reilley, C. N.; Van Duyne, R. P. *Anal. Chem.* **1972**, *44*, 142.

(19) Gagne, R. R.; Koval, C. A.; Lisensky, G. C. *Inorg. Chem.* **1980**, *19*, 2855.

(20) Chang, J. P.; Fung, E. Y.; Curtis, J. C. *Inorg. Chem.* **1986**, *25*, 4233.

(21) Callahan, R. W.; Brown, G. M.; Meyer, T. J. *Inorg. Chem.* **1975**, *14*, 1443.

(22) Aquino, M. A. S.; Bostock, A. E.; Crutchley, R. J. *Inorg. Chem.* **1990**, *29*, 3641.

Preparation of 1,4-Dicyanamidobenzene (DicydH₂). Benzoyl chloride (14 g, 0.1 mol) in 100 mL of acetone was added dropwise to a refluxing solution of ammonium thiocyanate (7.6 g, 0.1 mol) in 100 mL of acetone. The mixture was refluxed for an additional 5 min, and then 1,4-phenylenediamine (5.4 g, 0.05 mol) in 100 mL acetone was added dropwise. After addition was complete, the reaction mixture was refluxed for 15 min, and then the white thiourea derivative was filtered and washed with acetone, copiously with water, and then with acetone again. Crude yield is 93%.

The dry thiourea derivative (20.3 g, 0.0465 mol) was added to 250 mL of 2.5 M NaOH. The mixture was brought to a boil for 10 min and then cooled to 65 °C. Desulfurization of thiourea derivative was achieved by the addition of a solution of lead acetate trihydrate (37.9 g in 100 mL of water). The reaction mixture was stirred at approximately 65 °C for 5–10 min until it had turned a deep black with the precipitation of lead sulfide. The lead sulfide was filtered from the solution, and to the filtrate, cooled in an ice bath, was added 30 mL of glacial acetic acid. The white product which formed was filtered and washed copiously with water and then vacuum dried. The crude product was recrystallized from 50/50 acetone/water solution: yield 62%; mp dec > 182 °C.

Preparation of the Tetraphenylarsonium Salt of Dicyd²⁻, [AsPh₄]₂-[Dicyd]. DicydH₂ (0.5 g) and NaOH (3 g) were placed in a 100-mL, round-bottom flask and purged with argon. Previously degassed water (30 mL) was transferred under argon to the reaction flask, and the mixture was stirred until complete dissolution. [AsPh₄][Cl]·H₂O (2.6 g) was dissolved into 30 mL of 2.5 M NaOH aqueous solution. This solution was degassed and then transferred under argon to the basic solution of the ligand. The resulting yellow precipitate was filtered, washed with ice cold water, and then vacuum dried. The final red product was air sensitive and hygroscopic: yield 66%.

Preparation of the Tetraphenylarsonium Salt of Me₂Dicyd²⁻, [AsPh₄]₂[Me₂Dicyd]. The procedure is identical to the synthesis of [AsPh₄]₂[Dicyd]: yield 73%.

Preparation of the Tetraphenylarsonium Salt of Cl₂Dicyd²⁻, [AsPh₄]₂[Cl₂Dicyd]. This was prepared in a similar manner to [AsPh₄]₂[Dicyd] except that a molar ratio of 4:1 benzoylisothiocyanate to 2,5-dichlorophenylenediamine was used in the preparation of neutral ligand, Cl₂DicydH₂: yield 84%.

Preparation of 1, [μ-(1,4-Dicyanamidobenzene)bis|pentaammineruthenium(III)|] Tetraperchlorate Tetrahydrate, [μ-Dicyd-|(NH₃)₅Ru|₂][ClO₄]₄·4H₂O. The procedure for complex preparation is identical to that for the Cl₄Dicyd analogue.[22] Purification of the crude bromide salt (0.385 g) of the dinuclear complex was achieved by cation exchange chromatography using Sephadex C25-120 resin in a 2.5 × 30 cm column and eluting with 1 M NaCl solution. The eluent from the blue-green product band (approximately 80 mL) was added to a filtered solution of 10 g of sodium perchlorate (caution: perchlorate salts are potentially explosive and only small quantities of these complexes should be prepared)[24] and then placed in a refrigerator. The complex perchlorate salt crystallized readily from the cold solution and was filtered, washed with ice cold water, and then vacuum dried. The product was then recrystallized by ether diffusion into an acetone/water (10/1) solution of the product: yield 0.060 g (15%). Anal. Calcd for C₈H₄₂N₁₄O₂₀Cl₄Ru₂: C, 9.62; H, 4.24; N, 19.64. Found: C, 9.75; H, 4.06; N, 19.26.

Preparation of 2, [μ-(1,4-Dicyanamido-2,5-dimethylbenzene)bis|pentaammineruthenium(III)|] Tetraperchlorate, [μ-Me₂Dicyd-|(NH₃)₅Ru|₂][ClO₄]₄·¹/₆acetone. This complex was prepared in a similar manner to the Dicyd analogue. Recrystallization of the perchlorate salt by ether diffusion into an acetone/water (100:1) solution of the dinuclear complex yielded 80 mg (18%). Anal. Calcd for C₁₀.₅H₃₉N₁₄O₁₆.₁₆Cl₄Ru₂: C, 13.08; H, 4.08; N, 20.34. Found: C, 13.06; H, 3.97; N, 20.12.

Preparation of 3, [μ-(1,4-Dicyanamido-2,5-dichlorobenzene)bis|pentaammineruthenium(III)|] Tetrachloride, [μ-Cl₂Dicyd-|(NH₃)₅Ru|₂][Cl]₄·3H₂O. This complex was prepared in a similar manner to the Dicyd analogue. Elution from the cation exchange column required the use of 2.0 M NaCl to isolate the desired product. The eluent's volume (220 mL) was reduced under vacuum to approximately 100 mL and then stored at 4 °C overnight. The crystalline product was filtered off and washed with ice cold water. The product was recrystallized out of water by acetone diffusion: yield 17%. Anal. Calcd for C₈H₃₈N₁₄O₃Cl₆Ru₂: C, 12.11; H, 4.79; N, 24.71. Found: C, 12.23; H, 4.58; N, 24.58.

The dinuclear complexes were sufficiently stable to handle in the open but could not be heated under vacuum to drive off the solvent of recrystallization without decomposition. As a precautionary measure, the complexes were stored for extended periods under argon at −16 °C.

(23) Naklicki, M. L.; Crutchley, R. J. *Inorg. Chem.* **1989**, *28*, 4226.
(24) *J. Chem. Educ.* **1985**, *62*, 1001.

Table I. Electrochemical Data of Free 1,4-Dicyanamidobenzene Dianion Derivatives[a] and Dinuclear Pentaammineruthenium Complexes 1–4[b]

species	$E_m^{\bullet}$[c]	E_{11}°	E_{12}°
[AsPh₄]₂[Dicyd]		−0.465	0.210
[AsPh₄]₂[Me₂Dicyd]		−0.545	0.095
[AsPh₄]₂[Cl₂Dicyd]		−0.175	0.465
[AsPh₄]₂[Cl₄Dicyd]		−0.025	0.570
1	−0.051	0.632	0.981
2	−0.073	0.539	0.912
3	−0.003	0.814	1.13
4	−0.033	0.892	1.03[d]

[a] Free ligand cyclic voltammetry performed in acetonitrile (0.1 M TBAH), approximately 1 mM in ligand, $T = 25$ °C and a scan rate of 100 mV/s. [b] Dinuclear complex cyclic voltammetry performed in aqueous solution (0.1 M NaCl), approximately 1 mM in complex, $T = 25$ °C and a scan rate of 100 mV/s. [c] Ru(III/II) couples are actually two one electron reduction steps that are so close together that they do not resolve into separate waves. Ligand reduction couples are one electron reduction steps. See the text for further description. [d] Only the anodic peak is observed.

Crystallographic Studies of [μ-Dicyd-|(NH₃)₅Ru|₂][OTs]₄·acetone. Black rectangular cubic crystals of the complex were grown by acetone diffusion into an aqueous solution of the complex.

A summary of crystal data for the complex is given in Table II. The diffraction intensities were collected on a Nonius diffractometer at 295 with 1.54056 Å radiation by using the $\theta/2\theta$ scan technique with profile analysis.[25] The space groups were determined during the analysis. Unit cell parameters were obtained by least squares refinement of the setting angle for 19 reflections with 2θ angle in the range 80–100°. Corrections were made for absorption. The minimum and maximum transmission factors are 0.226 050 and 0.413 126, respectively.

The structure was solved by direct method and refined by full matrix least squares. Hydrogen atom positions were calculated. All the calculations were performed with the NRCVAX Crystal Structure Package.[26] The atomic parameters, anisotropic thermal parameters, final structure factors, and the complete full listing of bond lengths and angles are available as supplementary data.

Extended Hückel Calculations. These were performed with the Quantum Chemistry Program Exchange program No. QCMP 011, Forticon 8 for personal computers. Tables of atomic coordinates in Cartesian space are available as supplementary material.

Results

Crystal structure determinations of the tetraphenylarsonium salts of the ligands Dicyd²⁻, Me₂Dicyd²⁻ Cl₂Dicyd²⁻, and Cl₄Dicyd²⁻ have been performed and will be reported elsewhere.[27] In all cases, the ligands are planar with cyanamide groups in an anti configuration and linear (NCN bond angles range from 168.8 to 177.9°).

The π coupling between the anionic cyanamide groups and the phenyl ring that maintains the planar geometry of the dianion in the solid state is weak, and in solution rotation of the cyanamide group out of the plane of the phenyl ring is expected to occur. It has been shown that the activation energy for syn/anti isomerization of various dicyanoquinonediamine derivatives (two electron oxidation product of Dicyd²⁻ derivatives) is in the range of 13–17 kcal mol⁻¹.[28] Due to the partial double bond character of the phenyl carbon–cyanamide bond in Dicyd²⁻ derivatives, the activation energy to rotation for these compounds should be even less. We examined the ¹³C NMR spectrum of [AsPh₄]₂[Cl₂Dicyd] in methanol-d_4 down to −60 °C and observed the gradual broadening and coalescence of the cyanamide resonance. From this limited data, the energy barrier to rotation about the phenyl ring carbon–cyanamide bond was estimated to be ≤9 kcal mol⁻¹. It can therefore be assumed that while solid state conditions appear to favor a planar Dicyd²⁻ geometry with cyanamide groups in an

(25) Grant, D. F.; Gabe, E. J. *J. Appl. Crystallogr.* **1978**, *11*, 114.
(26) Gabe, E. J.; Lee, F. L.; Lepage, Y. *J. Appl. Crystallogr.* **1989**, *22*, 384.
(27) Aquino, M. A. S.; Lee, F. L.; Gabe, E. J.; Crutchley, R. J. To be submitted for publication.
(28) Aumuller, A.; Hunig, S. *Liebigs Ann. Chem.* **1986**, 142.

Table II. Crystal Data for $[\{(NH_3)_5Ru\}_2(\mu\text{-Dicyd})][OTs]_4\cdot$acetone

formula	$Ru_2S_4O_{13}N_{14}C_{39}H_{60}$
m wt	1263.35
cryst syst	monoclinic
space group	$P2_1/c$
a, Å	7.5861 (6)
b, Å	23.0450 (19)
c, Å	32.078 (3)
β, deg	95.771 (7)
V, Å^3	5579.5
Z	4
D_c, g/cm^3	1.504
cryst dimens, mm^3	0.20 × 0.20 × 0.10
radiation (λ, Å)	Cu (1.54056)
lin abs. coeff (μ, mm^{-1})	6.33
no. or reflns measd	5746
no. of unique reflns	5728
no. sig reflns	3947
R factor^a	0.063
R_w factor^a	0.048
goodness-of-fit ratio	3.71

$^a R = \sum||F_o| - |F_c||/\sum|F_o|$; $R_w = (\sum w(|F_o| - |F_c|)^2/\sum w|F_o|^2)^{1/2}$.

anti configuration, a number of conformations may exist in equilibrium for Dicyd^{2-} derivatives in solution.

Cyclic voltammetry data of the dianion ligands in acetonitrile are given in Table I. The results can be understood according to

Scheme I

$$L^{2-} \underset{}{\overset{-e^-}{\rightleftharpoons}} L^{\bullet-} \underset{}{\overset{-e^-}{\rightleftharpoons}} L$$
$$E^0_{11} \qquad E^0_{12}$$
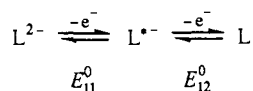
The E^0_{11} reduction couple appeared reversible (a peak to peak separation of 60 mV, independent of scan rate). The E^0_{12} reduction couple appeared quasi-reversible at best (peak-to-peak separation >80 mV at 100 mV s^{-1}, increasing with scan rate). In all cases, the anodic-to-cathodic current ratios at a scan rate of 100 mV s^{-1} were close to unity. The four ligands span a range of 0.52 V for E^0_{11} and 0.48 V for E^0_{12} and should offer an opportunity to study the dependence of coupling on the energy of the bridging ligand's HOMO provided other factors can be kept constant.

Crystal structure studies have all shown the planarity of a number of phenylcyanamido ligands to be unaffected by coordination to either Ru(III),[6] Cu(II),[29] or Cu(I),[30] and we felt it likely that the planarity of the Dicyd^{2-} bridging ligands would not be perturbed upon coordination to the Ru(NH$_3$)$_5$ moieties. Nevertheless, the establishment of planar geometry of the bridging ligand in one of the complexes in this study was deemed essential for a realistic theoretical analysis. Crystal growth of these dinuclear complexes is not a trivial matter as they are prone to dendrite and cluster formations. Success was achieved with the complex, $[\{(NH_3)_5Ru\}_2(\mu\text{-Dicyd})][OTs]_4\cdot$acetone, where OTs is the tosylate anion.

Figure 1 shows the structure of $[\{(NH_3)_5Ru\}_2(\mu\text{-Dicyd})][OTs]_4$, and Figure 2 shows the relative orientations of the complex salt and acetone within the unit cell. The crystal data and atomic positional parameters are given in Tables II and III, respectively. Selected bond lengths and angles are given in Table IV. The refinement of this crystal structure was reasonable with the unweighted residual (R_f) for the significant reflections being 6.3%. The unit cell was quite large having a volume of 5580 Å^3. As can be seen in Figure 1, there are two coordination isomers of **1**: a "linear" form **A** in which the Ru(1)–N(6)–C(1) bond angle is 175° and a "bent" form **B** in which the corresponding bond angle is only 150°. This result was surprising since a previous crystal

Table III. Atomic Parameters and $B_{iso}{}^a$ for $[\{(NH_3)_5Ru\}_2(\mu\text{-Dicyd})][OTs]_4$

	x	y	z	$B_{iso}{}^b$
Ru(1)	0.97921 (15)	0.84318 (5)	0.16553 (4)	3.03 (6)
Ru(2)	0.47067 (16)	0.56419 (5)	0.19502 (4)	3.92 (7)
N(1)	0.7062 (13)	0.8482 (4)	0.1666 (3)	3.22 (25)
N(2)	1.0122 (13)	0.9318 (4)	0.1820 (3)	3.5 (3)
N(3)	0.9483 (13)	0.7553 (4)	0.1490 (3)	3.25 (25)
N(4)	1.2620 (14)	0.8350 (5)	0.1650 (3)	3.6 (3)
N(5)	1.0025 (15)	0.8191 (4)	0.2302 (3)	3.9 (3)
N(6)	0.9512 (14)	0.8670 (4)	0.1073 (3)	3.3 (3)
N(7)	0.8912 (14)	0.8965 (5)	0.0341 (4)	4.3 (3)
N(8)	0.6705 (14)	0.6072 (4)	0.1646 (3)	4.1 (3)
N(9)	0.2659 (14)	0.6192 (5)	0.1683 (3)	4.9 (3)
N(10)	0.6763 (14)	0.5118 (5)	0.2247 (3)	4.7 (3)
N(11)	0.2780 (17)	0.5158 (6)	0.2262 (4)	4.3 (3)
N(12)	0.5007 (15)	0.6243 (5)	0.2446 (4)	4.1 (3)
N(13)	0.4339 (17)	0.5137 (5)	0.1454 (4)	5.6 (3)
N(14)	0.3110 (19)	0.4967 (6)	0.0724 (5)	7.7 (4)
C(1)	0.9280 (19)	0.8845 (6)	0.0736 (5)	4.2 (4)
C(2)	0.9485 (17)	0.9479 (6)	0.0184 (4)	3.4 (3)
C(3)	0.8906 (17)	0.9617 (6)	−0.0234 (4)	3.5 (3)
C(4)	1.0614 (18)	0.9865 (6)	0.0410 (4)	4.1 (3)
C(5)	0.3868 (24)	0.5077 (8)	0.1092 (6)	6.9 (5)
C(6)	0.422 (3)	0.4990 (7)	0.375 (6)	6.6 (5)
C(7)	0.3195 (24)	0.4879 (8)	−0.0007 (7)	8.6 (6)
C(8)	0.586 (3)	0.5126 (7)	0.0392 (5)	6.7 (5)

^{a}Estimated standard deviations are in parentheses. $^b B_{iso}$ is the mean of the principal axes of the thermal ellipsoid, Å^2.

Table IV. Selected Bond Lengths (Å) and Angles (deg)^a for $[\{(NH_3)_5Ru\}_2(\mu\text{-Dicyd})][OTs]_4$

Ru(1)–N(1)	2.078 (10)	N(1)–Ru(1)–N(2)	92.0 (4)
Ru(1)–N(2)	2.118 (10)	N(1)–Ru(1)–N(4)	178.1 (4)
Ru(1)–N(5)	2.138 (11)	N(1)–Ru(1)–N(6)	89.2 (4)
Ru(1)–N(6)	1.938 (11)	N(2)–Ru(1)–N(3)	179.6 (4)
Ru(2)–N(8)	2.129 (10)	N(2)–Ru(1)–N(6)	88.1 (4)
Ru(2)–N(9)	2.119 (11)	N(5)–Ru(1)–N(6)	177.9 (4)
Ru(2)–N(10)	2.121 (11)	N(8)–Ru(2)–N(10)	86.9 (4)
Ru(2)–N(11)	2.161 (12)	N(8)–Ru(2)–N(11)	176.5 (5)
Ru(2)–N(12)	2.103 (11)	N(8)–Ru(2)–N(13)	87.4 (5)
Ru(2)–N(13)	1.969 (13)	N(9)–Ru(2)–N(10)	177.0 (4)
N(6)–C(1)	1.515 (19)	N(10)–Ru(2)–N(13)	93.7 (5)
N(7)–C(1)	1.298 (19)	N(12)–Ru(2)–N(13)	174.8 (5)
N(7)–C(2)	1.376 (17)	Ru(1)–N(6)–C(1)	175.1 (10)
N(13)–C(5)	1.188 (24)	Ru(2)–N(13)–C(5)	149.8 (12)
N(14)–C(5)	1.28 (3)	N(6)–C(1)–N(7)	171.5 (15)
N(14)–C(6)	1.468 (23)	C(1)–N(7)–C(2)	119.7 (12)
C(2)–C(3)	1.406 (20)	N(7)–C(2)–C(3)	117.6 (12)
C(2)–C(4)	1.386 (20)	N(7)–C(2)–C(4)	124.2 (13)
C(3)–C(4)a	1.386 (20)	C(3)–C(2)–C(4)	118.2 (12)
C(6)–C(7)	1.40 (3)	C(2)–C(3)–C(4)a	120.8 (12)
C(6)–C(8)	1.28 (3)	N(13)–C(5)–N(14)	169.6 (18)
C(8)–C(7)b	1.49 (3)	N(14)–C(6)–C(7)	110.5 (17)
Ru(1)–Ru(1)a	13.11 (10)	N(14)–C(6)–C(8)	127.2 (18)
Ru(2)–Ru(2)a	13.27 (11)	C(5)–N(14)–C(6)	117.1 (15)
Ru(1)–Ru(2)	7.61 (5)	C(7)–C(6)–C(8)	122.2 (17)
		C(6)–C(7)–C(8)b	116.9 (16)

^{a}The atom numbers are shown in Figure 1 and estimated standard deviations are in parentheses.

structure of the mononuclear complex, $[(NH_3)_5Ru(2,3\text{-}Cl_2pcyd)][SO_4]$, where 2,3-Cl$_2$pcyd = 2,3-dichlorophenylcyanamido, showed a corresponding bond angle of 171.4°.[6] In addition, the linear form is expected to maximize the π interaction between the π acid Ru(III) ion and π donor cyanamide group and be more stable. Consistent with the presence of two conformers in the solid state, the infrared spectrum of the tosylate salt of **1** showed two $\nu(NCN)$ bands at 2099 and 2082 cm^{-1}. Similar coordination forms have been observed in the crystal structure of [Cu(bipyridine)(2,3-Cl$_2$pcyd)$_2$],[29a] and again multiple $\nu(NCN)$ bands were observed in the solid state IR spectrum. The observation of only one $\nu(NCN)$ band in the solution IR spectrum of the above Cu(II) complex led the authors to conclude that crystal packing forces were sufficient to distort the copper–cyanamide bond angle. It is important to note that the infrared spectra of complexes **2**,

(29) (a) Crutchley, R. J.; Hynes, R.; Gabe, E. J. *Inorg. Chem.* **1990**, *29*, 4921. (b) Brader, M. L.; Ainscough, E. W.; Baker, E. N.; Brodie, A. M. *Polyhedron* **1989**, *8*, 2219.

(30) Ainscough, E. W.; Baker, E. N.; Brader, M. L.; Brodie, A. M.; Ingham, S. L.; Waters, J. M.; Hanna, J. V.; Healey, P. C. *J. Chem. Soc., Dalton Trans.* **1991**, 1243.
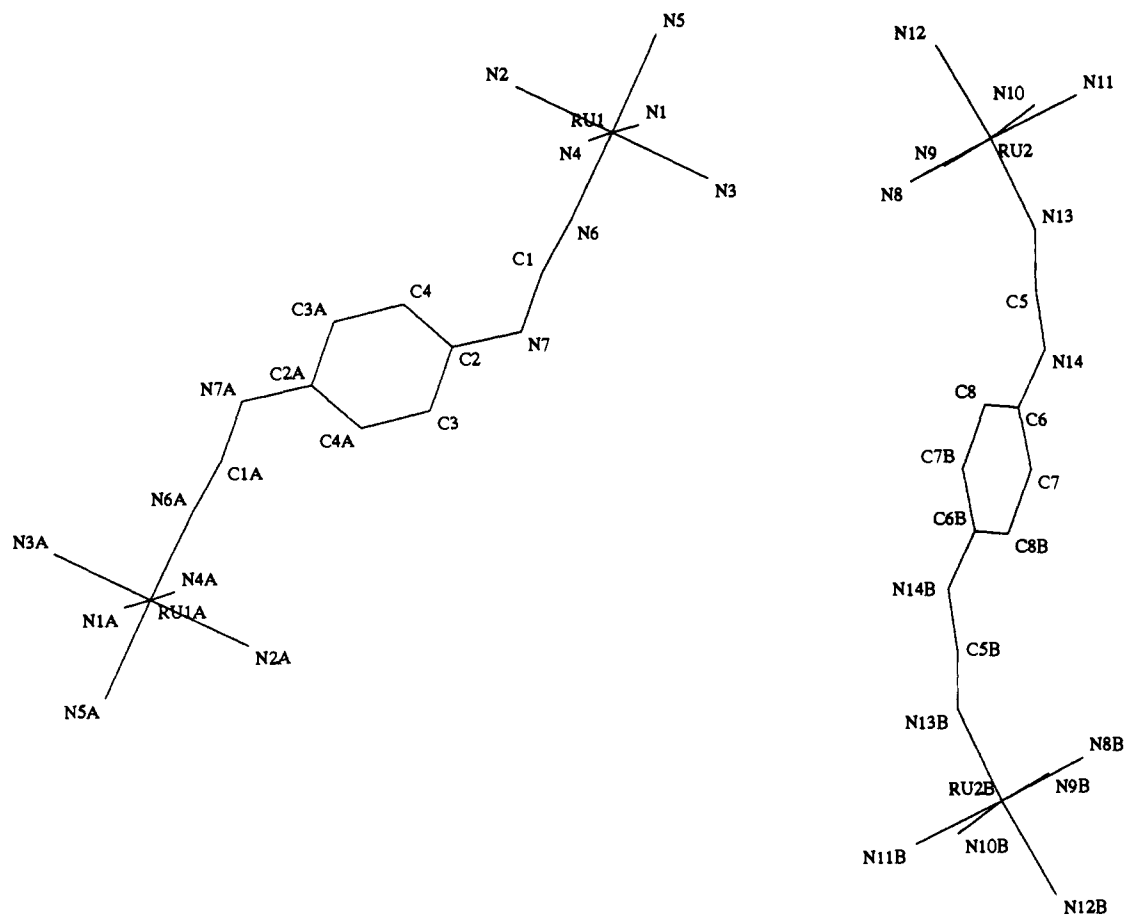
Figure 1. Crystal structures of the two conformers **A** and **B** of the dinuclear complex [μ-Dicyd-{(NH$_3$)$_5$Ru}$_2$][OTs]$_4$·acetone. The tosylate anion and acetone molecule have not been included for the sake of clarity.

Table V. Electronic Absorption[a] and Infrared[b] Spectroscopic Data of the Dinuclear Pentaammineruthenium Complexes 1–4

		LMCT		
complex	$\pi^* \leftarrow \pi$	$b_1{}^* \leftarrow b_2$	$b_1{}^* \leftarrow b_1$	ν(NCN)
1	211 (4.53), 266 (4.20) 345 (3.62)	385 (3.62)	865 (4.12) [0.35]	2087[c] 2082, 2099[d]
2	211 (4.53), 264 (4.26) 307 (3.85)	352 (3.70)	892 (4.20) 1046 (4.24) [0.42][e]	2088
3	216 (4.55), 272 (4.49) 320 (3.91)	376 (3.76)	803 (4.13) [0.33]	2098
4	225 (4.54), 278 (4.23) 325 (shoulder)	402 (3.67)	713 (3.93) [0.21]	2102

[a] In D$_2$O solution, data in nm (log ϵ M^{-1} cm^{-1}), square brackets enclose the total oscillator strength of low energy LMCT band for two Ru(III)-NCN chromophores per complex. [b] KBr disc, all bands were strong. [c] Perchlorate salt of complex 1. [d] Tosylate salt of complex 1. [e] Estimated combined oscillator strength of b$_1$* ← b$_1$ bands.

3, 4, and the ClO$_4^-$ salt of **1** all show a single ν(NCN) band (Table V). This is evidence for there being only one conformer in the solid state of these complexes.

The crystal structures of **1** and free Dicyd^{2-} ligand can be compared. The overall NCN bond length and CN bond lengths do not change significantly upon coordination. However, the bond that connects the cyanamide group to the phenyl ring does show some marked changes. In conformer **A**, N(7)–C(2) is 1.38 Å which is close to that of the free Dicyd^{2-} value of 1.39 Å. The corresponding bond in conformer **B**, N(14)–C(6), is much longer at 1.47 Å and indicates little if any double bond character.[31] In addition, the phenyl ring carbon–carbon bond lengths found in conformer **A** are quite similar to those of the free ligand and range from 1.39 to 1.40 Å, while those of conformer **B** show significant distortion and range from 1.28 Å C(6)–C(8) to 1.49 Å.

(31) Typical N–C single bonds are 1.47 Å. *Handbook of Chemistry and Physics* 64th ed.; Weast, R. C., Ed.; CRC Press: Boca Raton, FL, 1980; p F-217.

The ruthenium ions in both dimer types are in essentially octahedral environments. None of the N–Ru–N angles deviate by more than 4° from a right angle. The ruthenium–cyanamide bond in **A** Ru(1)–N(6) is 1.94 Å and in **B** Ru(2)–N(13) is 1.97 Å compared with a value of 1.98 Å in the crystal structure of [(NH$_3$)$_5$Ru(2,3-Cl$_2$pcyd)]$^{2+}$.[6] There does not appear to be any significant trans effect on the ammine trans to the cyanamide since all of the ruthenium–ammine nitrogen bonds in both forms are quite similar, ranging from 2.08 to 2.16 Å.

Our main assumption concerning the geometry of the Dicyd^{2-} bridging ligand was validated by the crystal structure of **1**. In both **A** and **B** conformers, the Dicyd^{2-} ligand is nearly planar, and the cyanamide groups are in an anti configuration. However, when the Ru(III) ions are included, only conformer **A** appears to have the optimal geometry for coupling via the π system of the bridging ligand. For conformer **A**, the best plane formed by N(6), Ru(1), N(2), N(5), and N(3) is tilted only 12° with respect to the plane of the phenyl ring carbons. The same dihedral angle for conformer **B** is 30° and planarity is essentially lost. The key difference in

Figure 2. Stereoview of the unit cell of the complex [μ-Dicyd-{(NH$_3$)$_5$Ru}$_2$][OTs]$_4$·acetone.

this form is the nonlinearity of the Ru(2)–N(13)–C(5) bond angle.

Finally, the intra- and intermolecular metal–metal distances should be mentioned. For conformer **A**, the Ru(1)–Ru(1)a through bond distance is 15.7 Å and the through space distance is 13.1 Å. For conformer **B**, the Ru(2)–Ru(2)b through bond distance is 15.9 Å and the through space distance is 13.3 Å. The shortest intermolecular distance occurred between Ru(1) and Ru(2) at 7.6 Å.

The UV–vis NIR spectral data of the four complexes are given in Table V. The spectrum of **4** has already been published.[22] An extensive discussion on the individual band assignments has appeared elsewhere for mononuclear phenylcyanamidopenta-ammineruthenium(III) complexes,[17] and similar arguments should apply to the dinuclear complexes of this study.

Unlike the majority of mononuclear pentaammineruthenium-(III) phenylcyanamide complexes,[6] the spectra of **1**, **2**, and **3** show splitting of the low-energy LMCT band. Since the LMCT transition is singly degenerate, it is suggested that this is evidence for a conformer equilibrium in solution. This equilibrium could be made up of the bent and linear ruthenium coordination conformers found in the crystal structure of **1** or if the cyanamide groups of the bridging ligand are free to rotate, syn and anti in-plane and out-of-plane bridging ligand conformations. A preliminary experiment over a temperature range of 6.5–86.5 °C resulted in spectral changes in the low energy LMCT band that were consistent with a conformer equilibrium. However, the data are not conclusive, and it will be necessary to extend the low temperature range.

The single electron reduction product of complex **1**, **2**, **3**, or **4** is a mixed valence [Ru(III), Ru(II)] system. If electronic coupling is significant, a metal-to-metal charge-transfer (MMCT) band should be present in the electronic spectrum. For the mixed-valence complex of **1**, **2**, and **3** no MMCT band could be discerned, and this was probably due to the intensity and proximity of the low energy LMCT band. However, for the previously reported mixed valence complex of **4**,[22] a MMCT band at 1220 nm ($\epsilon \leq$

Scheme II

$$(\text{Ru}^{II}, \text{L}^{2-}, \text{Ru}^{II}) \underset{\longleftarrow}{\overset{E^0_{M_1}}{\rightleftharpoons}} (\text{Ru}^{III}, \text{L}^{2-}, \text{Ru}^{II}) \underset{\longleftarrow}{\overset{E^0_{M_2}}{\rightleftharpoons}} (\text{Ru}^{III}, \text{L}^{2-}, \text{Ru}^{III})$$

$$\underset{E^*_M}{\underbrace{}}$$

$$(\text{Ru}^{III}, \text{L}^{2-}, \text{Ru}^{III}) \underset{\longleftarrow}{\overset{E^0_{L_1}}{\rightleftharpoons}} (\text{Ru}^{III}, \text{L}^{-}, \text{Ru}^{III}) \underset{\longleftarrow}{\overset{E^0_{L_2}}{\rightleftharpoons}} (\text{Ru}^{III}, \text{L}^0, \text{Ru}^{III})$$
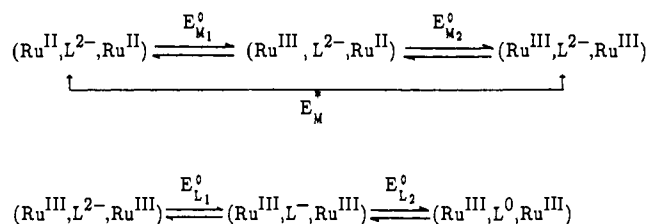
600 M^{-1} cm^{-1}) was sufficiently resolved from the low energy LMCT band to permit identification. Evidence for electronic coupling in all of the complexes can be found in the electrochemical studies and in the determination of comproportionation constants.

The cyclic voltammetry of complex **4** has already been discussed in detail[22] and is characteristic of the other complexes in this study. They all show similar patterns of one larger redox process followed by two smaller ones. These can be broken down as shown in Scheme II. The first process with a half wave potential defined as E_m^* is actually two closely overlapping one-electron transfer processes centered at the metals (i.e., consecutive Ru(III/II) couples, E^0_{m1} and E^0_{m2}). The smaller waves consist of ligand centered redox processes, E^0_{l1} and E^0_{l2}. The redox potentials are summarized in Table I.

In order to estimate the degree of electronic coupling in the mixed-valence complexes, the individual metal potentials must be determined. This means E_m^* must be resolved into two separate potentials, E^0_{m1} and E^0_{m2}, as defined by Scheme II. Once this has been accomplished, the comproportionation constant K_c (defined below) is easily determined from the difference in these two potentials.

Scheme III

$$[\text{Ru(III), Ru(III)}] + [\text{Ru(II), Ru(II)}] \overset{K_c}{\rightleftharpoons}$$
$$2[\text{Ru(III), Ru(II)}]$$
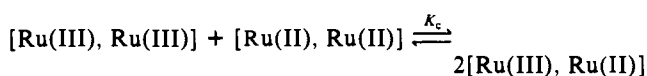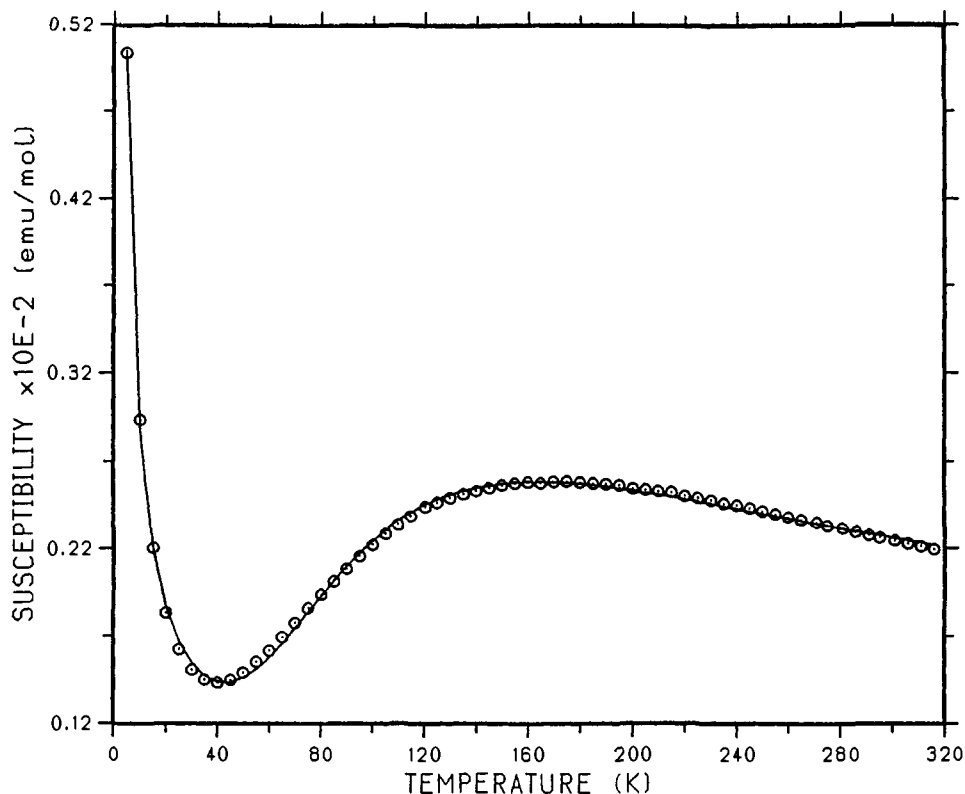
Figure 3. Experimental (○) and modelled (—) temperature dependences of the molar magnetic susceptibility of $[\mu\text{-}Cl_2\text{Dicyd-}\{(NH_3)_5Ru\}_2][ClO_4]_4$.

Table VI. Metal Centered Redox Potentials[a] and Comproportionation Constants for the Dinuclear Pentaammineruthenium(III) Complexes 1–4

complex	$\Delta E_p{}^b$	ΔE^c	$E_{m1}^\circ{}^d$	$E_{m2}^\circ{}^d$	$K_c{}^e$
1	85	60	−81	−21	10
2	120	85	−117	−32	28
3	110	78	−42	36	21
4	92	65	−67	−2	13

[a] All potentials in mV. [b] Anodic to cathodic peak separation of E_m^* in Table I. [c] Calculated potential difference between E_{m1}° and E_{m2}°, see text and ref 34. [d] Versus NHE and defined in Scheme II of text. [e] Defined in Scheme III of text.

Myers and Shain[32,33] have developed a method of determining ΔE° (the calculated separation between the individual metal redox couples, $E_{m2}^0 - E_{m1}^0$) from the experimentally determined values of $E_p - E_{p/2}$ (the difference between the peak potential and the half peak potential). The method can be used for both stationary-pulse voltammetry or cyclic voltammetry. Richardson and Taube[34] have extended this work and applied it to binuclear ruthenium pentaammines. The analysis requires that each separate redox process be reversible over a wide scan range, and the switching potential must be at least 250 mV beyond E_m^* to minimize peak distortion. In this study, the second criterion has been met and the first appears to be valid.

Table VI summarizes the calculated metal centered redox potentials and reports the comproportionation constants for the dinuclear complexes of this study. The values for K_c in Table VI are all less than 30 but at least greater than the statistical limit of 4. Similar low values of K_c were reported by researchers[35–37] for weakly coupled bipyridine bridged ruthenium pentaammine complexes.

Four factors[14] are important in determining the magnitude of the free energy of comproportionation ΔG_c: an entropic factor $(^1/_2 RT \ln{}^1/_4)$, an electrostatic factor, stabilization of the mixed-valence complex due to delocalization $(H_{ad}{}^2/E$, where E is the

energy at the MMCT band maximum), and finally a synergistic factor due to the stabilization of one metal oxidation state by the other. Taube and Sutton[36] showed that the value of $H_{ad}{}^2/E$ is small and that the major contributer to ΔG_c is the synergistic factor. Nevertheless, the bonding properties that promote a strong synergistic interaction between metal ions are much the same as those that increase the magnitude of H_{ad} and so the trend in K_c should roughly parallel the trend in H_{ad}.[36] Therefore, based on the trend in K_c in Table VI, the predicted trend in H_{ad} for the mixed-valence complexes is **2 > 3 > 4 > 1**.

Magnetic susceptibility measurements of the complexes were made over the temperature range 5–300 K. The high temperature range was restricted by instrumental limits but could not be increased in any case due to the thermal decomposition of the complexes (observed at temperatures >80 °C). The variation in molar magnetic susceptibility versus temperature of **3**, **4**, and the tosylate salt of **1** is shown in Figures 3, 4, and 5, respectively. Complexes **1** and **2** were also examined but were diamagnetic at room temperature and showed only a rapid rise in magnetic susceptibility at temperatures <40 K. This paramagnetic tail (seen also in Figures 3, 4, and 5) is usually ascribed to a monomer impurity, but for these dinuclear complexes an impurity due to oxidation of the dianion bridging ligand should also be taken into account. The broad maxima seen in Figures 3, 4, and 5 are characteristic of intramolecular antiferromagnetic exchange. Complexes **1** and **2** evidently undergo far stronger antiferromagnetic exchange with χ_{max} occurring at temperatures greater than 300 K. The possibility of intermolecular exchange can be discounted since it usually results in a phase transition to a long-range ordered state which gives rise to a sharp maximum at the transition temperature (Neel temperature). Intermolecular exchange is seen in monomeric Ru(III) complexes with similar ligands, but the effect occurs at much lower temperatures than those observed here.[38]

For the dinuclear systems of this study, both octahedral, low spin, Ru(III) ions have a $t_{2g}{}^5$ electron configuration, and so a single

(32) Meyers, R. L.; Shain, I. *Anal. Chem.* **1969**, *41*, 980.
(33) Polcyn, D. S.; Shain, I. *Anal. Chem.* **1966**, *38*, 37.
(34) Richardson, D. E.; Taube, H. *Inorg. Chem.* **1981**, *20*, 1278.
(35) Sutton, J. E.; Sutton, P. M.; Taube, H. *Inorg. Chem.* **1979**, *18*, 1017.

(36) Sutton, J. E.; Taube, H. *Inorg. Chem.* **1981**, *20*, 3125.
(37) Kim, Y.; Lieber, C. M. *Inorg. Chem.* **1989**, *28*, 3990.
(38) Carlin, R. L. *Magnetochemistry*; Springer-Verlag: Berlin Heidelberg, 1986.
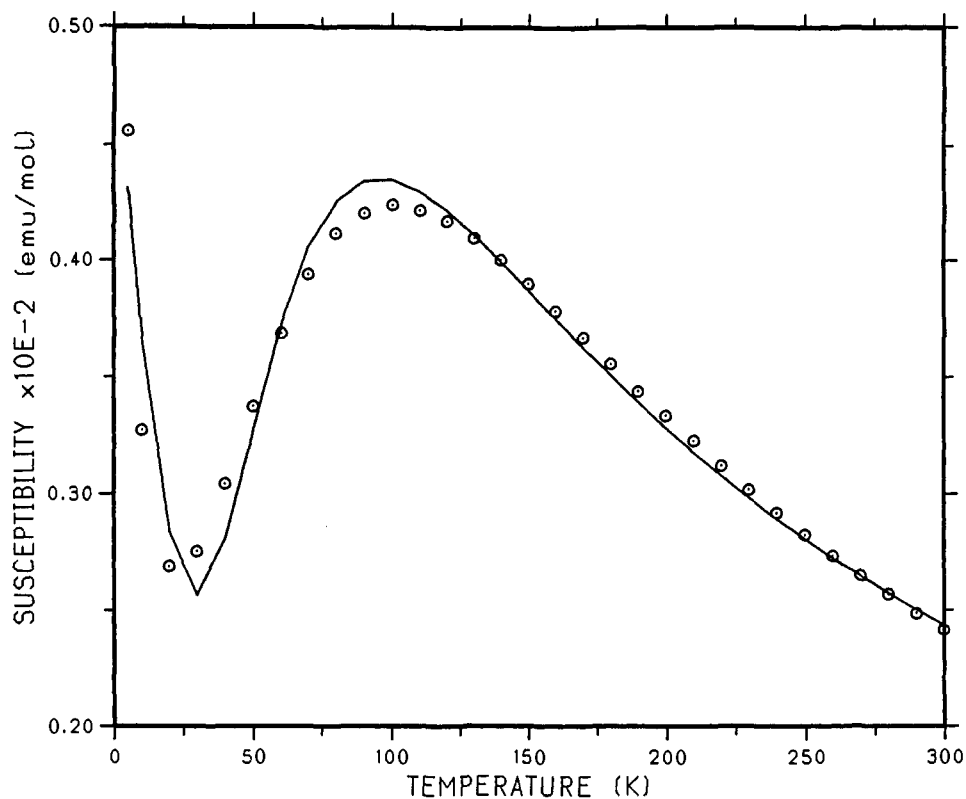
Figure 4. Experimental (⊙) and modelled (—) temperature dependences of the molar magnetic susceptibility of $[\mu\text{-Cl}_4\text{Dicyd-}\{(\text{NH}_3)_5\text{Ru}\}_2][\text{Cl}]_4$.
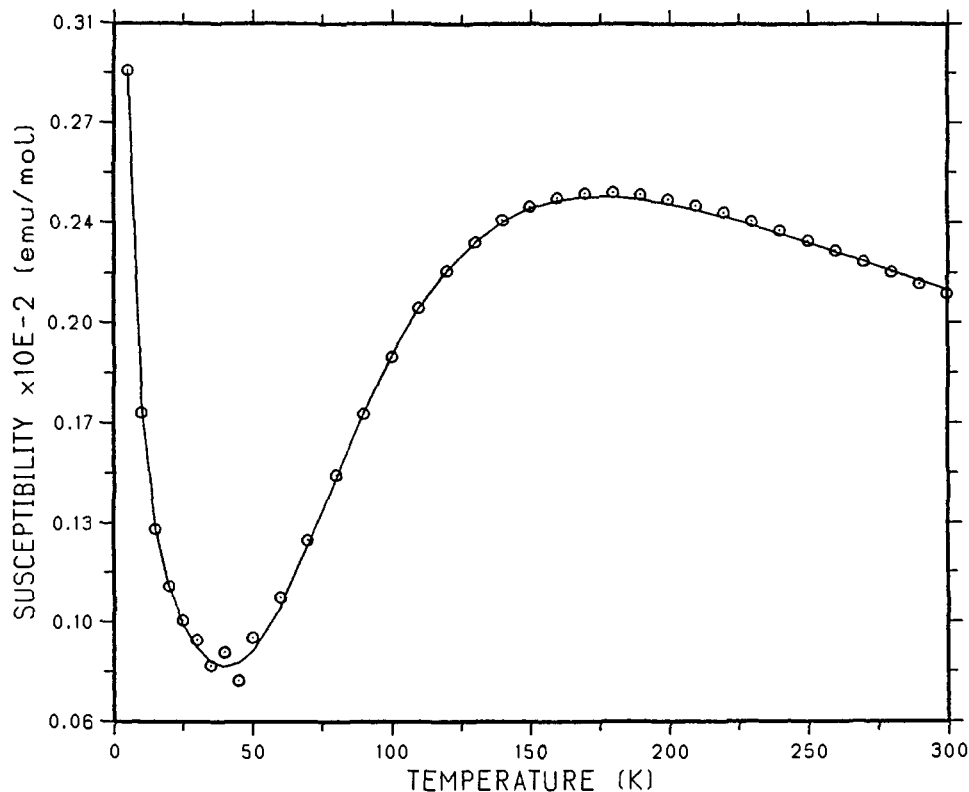
Figure 5. Experimental (⊙) and modelled (—) temperature dependences for the molar magnetic susceptibility of $[\mu\text{-Dicyd-}\{(\text{NH}_3)_5\text{Ru}\}_2][\text{OTs}]_4$.

unpaired electron occupies a π symmetry d-orbital on each metal ion. The treatment of the dependence of magnetic susceptibility on temperature is dominated by spin, but, for Ru(III), orbital angular momentum may make a significant contribution.[9] Drillon et al.[39] have developed procedures for including the orbital contribution for $t_{2g}{}^n$ configurations, but analytical expressions are not

available. Therefore, in order to get a good estimate of the exchange coupling constant, J, we have modelled our magnetic susceptibility data by assuming isotropically coupled, $S = {}^1/_2$ spins, and by using the modified Bleaney–Bowers expression[38]

$$\chi_m = C/(T - \theta) +$$
$$(2N\bar{g}^2\beta^2/3kT)[1 + ({}^1/_3)\exp(-2J/kT)]^{-1} + \chi_0 \quad (4)$$

where $\bar{g}$ is the powder average g value, $C/(T - \theta)$ is a Curie–Weiss

(39) Drillon, M.; Georges, R. *Phys. Rev. B* **1981**, *24*, 1278.

Table VII. Summary of Parameters which Gave the Best Fit of Magnetic Susceptibility Using Eq 4 for Complexes 1-4

complex	$\bar{g}$	$-J$ (cm^{-1})	C (emu cm^{-3} K^{-1})	θ (K)
(1)[ClO$_4$]$_4$		≤400		
(1)[OTs]$_4$	1.95	100	0.014	−0.651
(2)		≥400		
(3)	1.69	95.9	0.019	0.440
(4)	1.96	61.9	0.110	−21.6

term that corrects for any paramagnetic impurity at low temperatures, and χ_0 is a correction for any background paramagnetism. The line drawn through the data points in Figures 3, 4, and 5 is the respective best fit of the parameters J, $\bar{g}$, C, θ, and χ_0 in the above equation, and these are summarized in Table VII. It should be noted that the $\bar{g}$ values fall in the range of typical Ru(III) complexes, however, they must be treated with caution since in the present data analysis, the main effect of the paramagnetic impurity will be to reduce $\bar{g}$ artificially.

The fit for complex **4** (Figure 4) is significantly poorer than the rest and this may be due to a g factor anisotropy. The data for this complex was therefore fitted to the highly anisotropic Ising model.[40,41] While this model gave an improved fit near χ_{max}, it was poorer at higher temperatures, and since no advantage was seen, the model was not investigated further.

The magnetic susceptibility data of the ClO$_4^-$ salt of complex **1** showed a very slight rise as the temperature approached 300 K. From this we have estimated $-J \leq 400$ cm^{-1}.

There are many examples of antiferromagnetic coupling between metal sites in which the J values have much the same range as those shown in Table VII.[42] What is unprecedented about antiferromagnetic coupling in complexes **1-4** is that it occurs at a separation between metal ions of approximately 13 Å and is of sufficient magnitude to render complexes **1** and **2** diamagnetic at room temperature. Understanding the mechanism of antiferromagnetic coupling in these unusual complexes requires a close examination of the nature of the superexchange pathway or pathways.

Discussion

In bridged dinuclear systems, metal–metal coupling is mediated by the full set of bonding and antibonding orbitals of the bridging ligand. The extent to which a given ligand orbital contributes to the overall interaction is governed by the magnitude of its orbital overlap with the coupled metal orbitals. Factors to be considered are the separation between metal and ligand orbitals, symmetry, and energy. The relative energies of metal and bridging ligand orbitals can be derived from theory and experimental data. Fundamentally important information can be obtained from electronic absorption spectroscopy if the dominant pathway for metal–metal coupling involves the same orbitals as those resulting in metal-to-ligand or ligand-to-metal charge-transfer transitions (MLCT or LMCT, respectively). In the discussion to follow, we take a simplified view of the overall coupling pathway and consider only the highest occupied (HOMO), second highest occupied (SHOMO), and lowest unoccupied (LUMO) molecular orbitals of the bridging ligand and the exchanged coupled dπ-orbitals of ruthenium in either 3+ or 2+ oxidation states. We will show that an optimum pathway for electron exchange is present in [Ru(III), Ru(III)] complexes, but for electron exchange in the mixed-valence [Ru(III), Ru(II)] complexes the coupling pathway is less clearly defined.

The crystal structure of complex **1** shows the ruthenium ions to be in a pseudooctahedral environment. For Ru(III) and Ru(II) ions with respective low spin d^5 and d^6 electron configurations, this constrains the electrons to π symmetry d-orbitals. Therefore,

(40) McCoy, B. M.; Wu, T. T. *The Two Dimensional Ising Model*; Harvard University Press: Cambridge, 1973.
(41) Nakasuka, S.; Osaki, K.; Uryu, N. *Inorg. Chem.* **1982**, *21*, 4332.
(42) *Magneto-Structural Correlations in Exchange Coupled Systems*; Willet, R. D., Gatteschi, D., Kahn, O., Eds.; Reidel: Dordrecht, Holland, 1985. Shepard, R. E.; Proctor, A.; Henderson, W. W.; Myser, T. K. *Inorg. Chem.* **1987**, *26*, 2440.
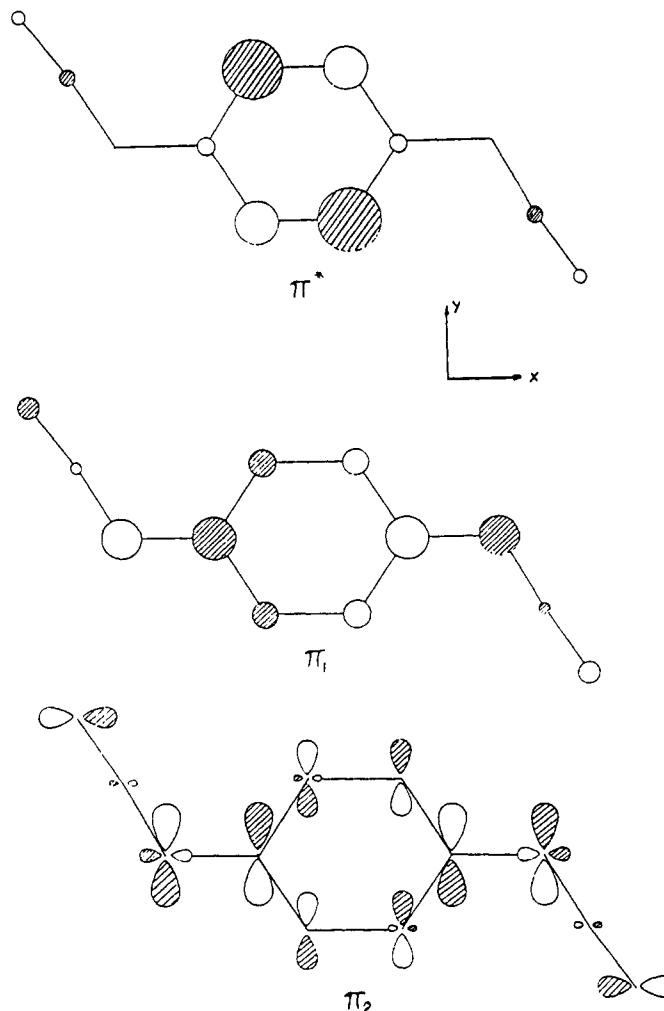
Figure 6. Frontier orbitals of Dicyd^{2-} from EHMO calculations. Minor orbital contributions are omitted for clarity.

effective electron exchange between ruthenium ions requires that there be a continuous π symmetry ligand MO that can interact simultaneously with both ruthenium ions. Extended Huckel calculations using the crystal structure data of the free dianion ligands[27] were performed in order to elucidate the properties of the π bonding and antibonding MOs of the bridging ligands. The electron density coefficients of the π MOs of the bridging ligands are basically the same with variations consistent with the nature of the substituents on the phenyl ring. Representative HOMO, SHOMO, and LUMO of the Dicyd^{2-} ligand are shown in Figure 6. Importantly, both the HOMO and SHOMO are continuous π MOs that span the entire bridging ligand and provide an energetically favorable pathway for superexchange.

In the crystal structure of **1** (Figure 1), two coordination isomers were observed. For conformer **A**, the dihedral angle between the best plane described by N(6), Ru(1), N(2), N(5), and N(3) atoms and the plane of the phenyl ring is only 12° and the Ru–NCN bond angle is 175°. In this case, the bridging ligand's HOMO has the optimum orientation to interact simultaneously with the exchanged coupled Ru(III) πd-orbitals as shown below.
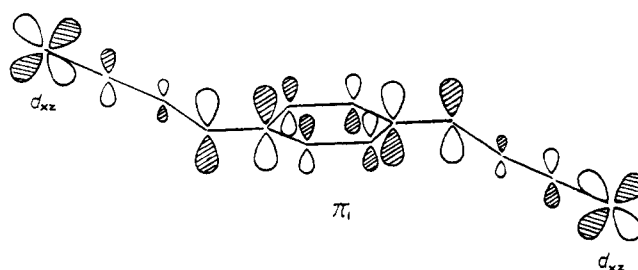
For conformer **B** with the bent Ru(III)–NCN bond and a 30° dihedral angle between the best planes of the phenyl ring and the N(13), Ru(2), N(8), N(11), and N(12) atoms, the bridging ligand's SHOMO has the proper orientation to interact simultaneously with the exchange coupled Ru(III) πd-orbitals as shown below.
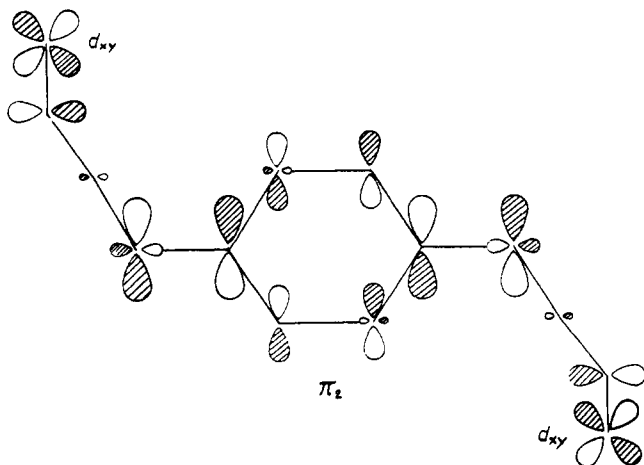
Thus, whether a complex adopts **A** or **B** conformations, a continuous, energetically favorable, π pathway between ruthenium ions is available. The result is the unprecedented magnitude of antiferromagnetic exchange (Table VII) observed for Ru(III) ions that are separated by 13.2 Å. The significance of these results should be placed into historical perspective.

In 1979, Coffman and Buettner[43] proposed the following limit function for the distance dependence of antiferromagnetic exchange between metal ions bridged by an insulating medium

$$|2J_{\lim}| = 1.35 \times 10^7 \exp(-1.80r) \quad \text{in cm}^{-1} \quad (5)$$

where r is the separation between metal ions in Å, the exponential value of -1.80 is a measure of the potential barrier to electron exchange in Å^{-1}, and the prefactor represents an arbitrary exchange "constant". The above relationship was derived by an empirical fit of literature data, and the parameters were justified after the fact. In addition, the expression represents a special case in which through bond electron exchange is suggested to be maximized with the only variable being the separation (or the number of bonds) between metal ions. As a limit function, the relationship has held up fairly well with some notable exceptions,[44,45] and for a given separation between metal ions the variation in J values between different dinuclear metal complexes can be treated by more sophisticated methods.[46] Nevertheless, the continued use of eq 5 by researchers[47] requires that its application be placed in context with the results of this study.

At a separation of 13.2 Å, eq 5 predicts $|2J| = 6.5 \times 10^{-4}$ cm^{-1}. The J values in Table VII are in complete disagreement with this result, and the breakdown of eq 5 is apparent. This breakdown arises because of a fundamental difference in the nature and properties of the electron exchange pathway in the complexes used to derive the Coffman–Buettner relationship compared to that of the complexes in this study.

The data used to derive eq 5 largely came from magnetic measurements of dinuclear Cu(II) complexes. For Cu(II), the odd electron resides in a mostly σ symmetry d-orbital, and electron

exchange is thought to predominantly occur via the σ bonding framework of the bridging ligand. The large difference in energy between the Cu(II) dσ-orbitals and the σ bonding electrons of the bridging ligand (>3 eV) is sufficient to classify the bridging ligand as an *insulating* medium with respect to electron exchange. For the complexes of this study, electron exchange pathway occurs via Ru(III) πd-orbitals and the π symmetry HOMO of the bridging Dicyd^{2-} ligand. The energy gap between these orbitals is relatively small (0.48–0.94 eV, for complex **2** and **4**, respectively), and we feel that the bridging ligand in these dinuclear Ru(III) complexes is more appropriately classified as a *semiconducting* medium.

The use of the terms insulating and semiconducting is deliberate as their connotations apply to the synthesis of molecular electronic devices. Indeed, the construction of a "molecular wire" has the requirement of no energy gap between those orbitals involved in electron exchange (i.e., a *conducting* medium).

The magnetic susceptibility data of complex **1** show a remarkable counter anion effect (Table VII). Counter anion variations in J are usually ascribed to intermolecular exchange interactions.[38,44a] However, in this case, $|\Delta J| \approx 300$ cm^{-1} which is far too large to be explained by relatively weak intermolecular interactions between octahedral Ru(III) ions.[48] A more likely explanation is that there exists a difference in the solid state complex structures between ClO$_4^-$ and tosylate complex **1** salts. We already know that the crystal structure of the tosylate salt of complex **1** showed two conformers which gave two ν(NCN) bands in the infrared spectrum. Since the infrared spectrum of the ClO$_4^-$ salt of complex **1** showed only a single sharp ν(NCN) band, it is tempting to suggest that only conformer **A** is present in this complex and that conformer **A** experiences greater antiferromagnetic coupling than does conformer **B**. A consequence of this rationale is that the observed magnetic susceptibility of the tosylate salt of complex **1** originates entirely with conformer **B**, conformer **A** being diamagnetic at the temperatures studied. However, this is not consistent with its reported value of $\bar{g} = 1.96$. This value is consistent with *all* of the $S = ^1/_2$ ions contributing to the paramagnetic susceptibility in this temperature range. If half of the Ru(III) ions were diamagnetic, the measured susceptibility near $T(\chi_{\max})$ would be nearly four times smaller. It seems likely that the only way to resolve this question is to obtain a crystal structure of the ClO$_4^-$ salt of complex **1**, and we hope to have one in the near future.

In order to understand the trends in antiferromagnetic coupling and comproportionation constants, it is helpful to construct an energy scheme (Figure 7) of the frontier MOs of the bridging ligands relative to the πd orbitals of Ru(II) and Ru(III). The relative energy separation between Ru(II) and Ru(III) d-orbitals can be estimated to be 2.6 eV from the photoelectron spectra of [Ru(NH$_3$)$_6$]Cl$_3$ and [Ru(en)$_3$]ZnCl$_4$, where en = ethylenediamine.[49] We have the relative energies of the frontier orbitals of the bridging ligand from extended Huckel calculations. The difference in energy, ΔE, between the Ru(III) πd-orbitals and the HOMO can be estimated from the lowest energy LMCT band energies (b$_1$* ← b$_1$) in Table V by using[6,50]

$$\Delta E = E_{op} - \chi \quad (6)$$

where E_{op} is the energy of the LMCT transition and χ is a correction to compensate for the change in inner and outer coordination sphere configurations resulting from a transition into an excited vibrational level of the excited state. We place a value on χ of 0.8 eV[51] and by using eq 6 and the data in Table V, the

(43) Coffman, R. E.; Buettner, G. R. *J. Phys. Chem.* **1979**, *83*, 2387.
(44) (a) Felthouse, T. R.; Hendrickson, D. N. *Inorg. Chem.* **1978**, *17*, 2636. (b) Francesconi, L. C.; Corbin, D. R.; Clauss, A. W.; Hendrickson, D. N.; Stucky, G. D. *Inorg. Chem.* **1981**, *20*, 2059.
(45) Chaudhuri, P.; Oder, K.; Wieghardt, K.; Gehring, S.; Haase, W.; Nuber, B.; Weiss, J. *J. Am. Chem. Soc.* **1988**, *110*, 3657.
(46) (a) Beratan, D. N.; Hopfield, J. J. *J. Am. Chem. Soc.* **1984**, *106*, 1584. (b) Onuchic, J. N.; Beratan, D. N. *J. Am. Chem. Soc.* **1987**, *109*, 6771.
(47) (a) Hendrickson, D. H. In ref 42, p 523. (b) Francesconi, L. C.; Corbin, D. R.; Clauss, A. W.; Hendrickson, D. N.; Sticky, G. D. *Inorg. Chem.* **1981**, *20*, 2059. (c) Verdaguer, M.; Gouteron, J.; Jeannin, Y.; Kahn, O. *Inorg. Chem.* **1984**, *23*, 4001. (d) Julve, M.; Verdaguer, M.; Faus, J.; Tinti, F.; Moratal, J.; Monge, A.; Gutierrez-Puebla, E. *Inorg. Chem.* **1989**, *26*, 3520.

(48) Bunker, B. C.; Drago, R. S.; Hendrickson, D. N.; Richman, R. M.; Kessell, S. L. *J. Am. Chem. Soc.* **1978**, *100*, 3805.
(49) Shepard, R. E.; Proctor, A.; Henderson, W. W.; Myser, T. K. *Inorg. Chem.* **1987**, *26*, 2440.
(50) Lever, A. B. P. *Inorganic Electronic Spectroscopy*, 2nd ed.; Elsevier Publishing Co.: Amsterdam, 1985, p 776.
(51) This value is the average of 0.61 eV, the intercept of the linear correlation between E_{op} and the difference between ligand and metal redox potentials for a series of pentaammineruthenium(III) phenylcyanamido complexes in ref 6 and 1.0 eV, the MMCT band energy of mixed-valence complex (**4**).
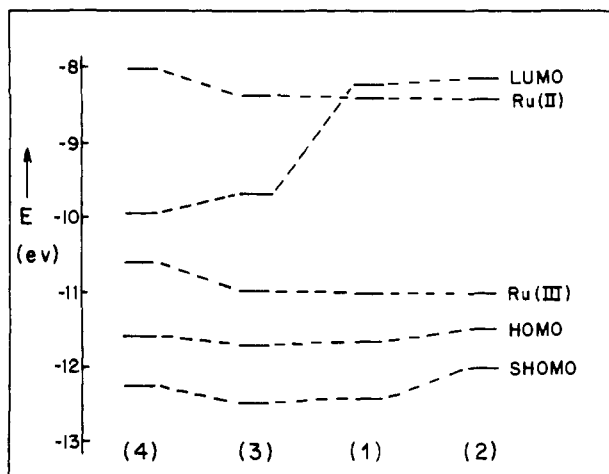
Figure 7. Qualitative energy level scheme of the frontier orbitals of complexes **1–4**.

relative energies of those orbitals important to electron exchange were derived and are shown in Figure 7.

By correlating the antiferromagnetic J values in Table VII with Figure 7, it is clear that an increase in antiferromagnetic coupling occurs with decreasing energy gap between HOMO and Ru(III) orbitals. In addition, the LMCT oscillator strength (Table V) which can be related to the overlap between HOMO and Ru(III) orbitals[6,7] also increases with decreasing energy gap. The above behavior reaffirms the semiconducting properties of the Dicyd^{2-} bridging ligands when bound to Ru(III).

For the mixed-valence [Ru(III), Ru(II)] complexes, the trend in K_c and by inference H_{ad}, $1 < 4 < 3 < 2$, does not follow the above trend since the exchange coupling for **1** is smaller than expected. We have shown that in solution there is little barrier to rotation of cyanamide groups about the phenyl ring. If the cyanamide groups rotate out of the phenyl ring plane, the HOMO becomes more localized in the phenyl ring, and this reduces its ability to couple with the Ru(III) πd-orbitals. This was illustrated by an extended Huckel calculation of the bridging ligand 1,2-dicyanamido-2,3,5,6-tetramethylbenzene dianion (Me$_4$dicyd^{2-}).[52] If the mixed-valence complex **1** undergoes free rotation of the cyanamide groups about the phenyl ring in solution, this would attenuate electron exchange via the bridging ligands π MOs and may explain the depressed value of K_c for **1**.

Ignoring the mixed-valence complex **1**, electron coupling in mixed-valence complex **2**, **3**, and **4** does follow the same trend as the trend in magnetic exchange. This suggests that the optimum pathway for electron exchange in the mixed-valence complexes involves the Ru(III) $d\pi$-orbitals and bridging ligand HOMO. However, the energy level of Ru(II) is sufficiently high to interact with the antibonding orbitals of the bridging ligands (Figure 7). We have no spectroscopic evidence for this interaction, but the very intense LMCT bands could very well obscure any MLCT transition. For the mixed-valence complexes, we conclude that while there is evidence for electron exchange via the bridging ligand HOMO, electron exchange via antibonding orbitals may make a significant contribution.

Since the electron exchange mechanisms in both mixed-valence [Ru(III), Ru(II)] and oxidized [Ru(III), Ru(III)] complexes at least partially share the same orbital pathway, it would be of interest to compare the electronic exchange integral H_{ad} found for the mixed-valence complexes with the electronic exchange integral H_{ab} determined from magnetic analysis.

Second order antiferromagnetic contributions have been shown to be important in ab initio calculations of exchange coupled copper(II) dimers.[52] However, these second order contributions

(52) Aquino, M. A. S.; Lee, F. L.; Gabe, E. J.; Crutchley, R. J. *Inorg. Chem.* **1991**, *30*, 3234.

(53) Daudey, J. P.; De Loth, P.; Malrieu, J. P. in ref 41, p 87.

become less important with increasing separation between metal ions as does the ferromagnetic term in eq 2. Indeed, when the large separation between Ru(III) ions in this study is considered, the ferromagnetic term may well be cancelled out by these second order antiferromagnetic contributions.[15] If so, it may be reasonable to simplify eq 2 to

$$2J \approx -(2H_{ab}{}^2)/J_{aa} - J_{ab} \qquad (7)$$

In order to estimate H_{ab} from the above expression, a value for $J_{aa} - J_{ab}$ must be determined. The expression $J_{aa} - J_{ab}$ represents the difference in energy between the ground state in which electrons are on separate metal ions and the excited state in which both electrons are localized on one metal ion. A good estimate is simply the difference in the PES d-orbital binding energies of [Ru(NH$_3$)$_6$][Cl]$_3$ and [Ru(en)$_3$][ZnCl$_4$],[49] and so $J_{aa} - J_{ab}$ was given a value of 2.6 eV. Substituting this value and the J values found in Table VII into eq 4 gives for complex **4**, $H_{ab} = 460$ cm^{-1}; for complex **3**, $H_{ab} = 590$ cm^{-1}; for the tosylate salt of complex **1**, $H_{ab} = 590$ cm^{-1}; for the ClO$_4^-$ salt of complex **1**, $H_{ab} < 1200$ cm^{-1}; for complex **2**, $H_{ab} \geq 1200$ cm^{-1}. These values of H_{ab} are significantly greater than those estimated for H_{ad} in the mixed-valence complexes. For [Ru(III), Ru(II)] complex **4**, H_{ad} was calculated by using eq 3 to be no greater than 185 cm^{-1}.[22] The trend in comproportionation constants for the mixed-valence complexes allows us to place an estimated maximum value of H_{ad} for complex **2** of 370 cm^{-1}. If our use of eq 7 is appropriate, the larger respective value of H_{ab} compared H_{ad} may be partially explained by the predominance in [Ru(III), Ru(III)] complexes of superexchange via $d\pi$-orbitals and the HOMO of the bridging ligand. In addition, the solid state geometry of the dinuclear complexes is expected to reflect the most stable conformation in which intramolecular interactions are maximized. In solution, the solid state geometry of the complexes is not expected to be maintained, resulting in attenuation of superexchange.

Summary and Conclusion

Long range antiferromagnetic exchange at a separation of approximately 13.2 Å between Ru(III) ions was observed for the [Ru(III), Ru(III)] complexes of this study. The magnetic exchange constant $-J$ ranged from 61.9 to ≥ 400 cm^{-1}. The unprecedented magnitude of J at this separation is due to a continuous and energetically favorable superexchange pathway involving the Ru(III) $d\pi$-orbitals and the π HOMO of the bridging Dicyd^{2-} ligand. Mixed-valence [Ru(III), Ru(II)] complexes did not show as strong a superexchange coupling as the [Ru(III), Ru(III)] complexes. It was suggested that the Ru(II) $d\pi$-orbitals, being higher in energy than the Ru(III) $d\pi$-orbitals, could not as readily couple with the preferred pathway for superexchange involving the HOMO of the bridging ligand. It is also probable that the geometry of a mixed valence complex is not as rigid in solution as it is in the solid state and that any distortion from ideal geometry would attenuate superexchange coupling.

Future studies will explore the dependence of superexchange coupling via a continuous π pathway on the separation between metal ions and the energy gap between exchange coupled orbitals and bridging ligand HOMO.